EUROPEAN ORGANIZATION FOR NUCLEAR RESEARCH

CERN–EP/2001–020
12 Juanary 2001

Low-lying levels in ^{119}Xe

J. Genevey, A. Gizon
Institut des Sciences Nucléaires, IN2P3 -CNRS/ Université Joseph Fourier
F-38026 Grenoble Cedex, France

P. F. Mantica, W. B. Walters
Department of Chemistry and Biochemistry, University of Maryland,
College Park, MD 20742, USA

G. Marguier
Institut de Physique Nucléaire IN2P3 -CNRS/ Université Claude Bernard Lyon-1
F- 69622 Villeurbanne, France

D. Bucurescu
Horia Hulubei National Institute of Physics and Nuclear Ingineering
R- 76900 Bucharest, Romania

and the ISOLDE collaboration
CERN, CH 1211 Geneva 23, Switzerland

ABSTRACT

The decays of ^{119m}Cs and ^{119g}Cs to ^{119}Xe have been studied on mass separated samples, using $\gamma-$ray and internal conversion electron measurements. Several new low-lying levels have been established in the ^{119}Xe level scheme. Half-life evaluations for ^{119m}Cs and ^{119g}Cs have been revisited. The results are compared with other experimental data known in light odd-mass xenon isotopes and with calculations performed in the frame of the multi-shell interacting boson-fermion model.

(PACS numbers : 23.20.Lv; 23.20.Nx; 27.60.+j.)

1 INTRODUCTION

The present study is part of a program developed at the ISOLDE facility to investigate the $\beta-$decay schemes of light cesium isotopes [1], [2]. The experiments have been focused on the ^{119}Xe low-lying level scheme populated in the β/EC decays of ^{119m}Cs and ^{119g}Cs for which a few results have been previously reported [3]. This approach is very similar to the one already applied for the ^{121m,g}Cs to ^{121}Xe beta decays [4].

Spin and parity of the ^{119}Xe ground-state are definitely known to be $I^{\pi} = 5/2^{+}$ [5]. A first partial level scheme for the lowest excited states fed by beta decay in ^{119}Xe has been reported to stand a comparison with the ^{117}Xe isotope [6]. From in-beam studies of ^{119}Xe a wealth of data is available at intermediate - and high-spin states [7], [8], [9], [10]. Negative-parity band structures having similar characteristics and based on a $\nu h_{11/2}$ quasineutron configuration have been reported by all works. The situation is significantly more complex for the low-spin positive-parity states. A comparison of the band structures developed in ^{119}Xe with those recently established in the neighbouring isotope ^{121}Xe [11], [12] shows clearly a similar behaviour for the $\Delta = 1$ bands built on the $\nu d_{5/2}[402]5/2^{+}$ ground-state of the two nuclei.

Additional experiments are needed to firmly establish the spin, parity assignments and deexcitation modes of the other low-lying states. Comparing the ^{121}Xe low-lying positive-parity states fed in the ^{121m,g}Cs beta-decays [4] and those with spin-parity $I^{\pi} \leq 11/2^{+}$ populated in the ^{109}Ag(^{16}O, p3n) reaction (bands $9-10$ and $11-12$ in [12]) one observes an interesting agreement. Keeping this similarities in mind, a special effort has been made in the present ^{119m,g}Cs beta-decay study to establish the spin and parity assignments of the low-lying states fed in ^{119}Xe and to combine them with those proposed from recent in-beam $\gamma-$ray spectroscopy studies [9], [10].

In section 2 of this paper the experimental procedures and the results are reported. The level scheme is established in section 3 and the $\beta-$feedings in section 4. The discussion of the new results is presented in the last part, including comparisons with other experimental data and with calculations performed in the frame of the interacting boson-fermion model (IBFM).

2 EXPERIMENTAL PROCEDURES AND RESULTS

The present study of the β/EC decay of ^{119m,g}Cs to levels in ^{119}Xe was completed in part at the ISOLDE facility at CERN and at the UNISOR isotope separator at Oak Ridge National Laboratory (ORNL).

In the studies at ISOLDE, cesium isotopes were produced in a thick molten lanthanum target bombarbed by the 600 MeV proton beam available at CERN. The experimental set-up was similar to the one described in a previous paper on the ^{121m,g}Cs decay [4]. Separated radioactive samples were collected during various collecting times in the 1 to 30 seconds range, and sequentially transported to the counting station by an automatic tape driver system. The counting times were typically of 30 seconds. Singles $\gamma-$ray spectra and time-dependent multiscaling spectra were recorded with an intrinsic Ge detector having a resolution of 800 eV at 122 keV for the low-energy $\gamma-$rays and with several other Ge(Li) coaxial detectors (15% efficiency and $R \approx 2.5$ keV at 1 MeV).

Conversion electron spectra were detected with a movable 3 mm thick Si(Li) detector having a resolution of 1.6 keV FWHM at 624 keV and placed in the vacuum,near the collected samples. Three parameter $\gamma-\gamma-$t and $\gamma-$e $-$ t coincidence events have been recorded. For $\beta^{+}-\gamma$ coincidence measurements, a typical arrangement including a $4\pi\beta$

plastic scintillator and a Ge(Li) detector has been used. This disposal is of the same type as the one used at the TRISTAN mass separator [13].

In the studies at UNISOR, samples of ^{119}Cs were produced in the heavy-ion reaction between a 6 mg/cm^2 ^{92}Mo target, which made the window of the FEBIAD-B2 ion source [14], and a 175 MeV ^{32}S beam provided by the 25 MV Tandem accelerator at the Holifield Heavy Ion Research Facility at ORNL. The evaporation products from the heavy-ion reaction recoiled in the center of the ion source, where they were ionized to a singly-positive charge and extracted towards the mass separator. The recoil ions were then mass separated, and the ^{119}Cs products were deposited into a moving tape, which transported the activity to two counting stations with a cycle time of 40 seconds. The first counting station (G1) consisted of two $\gamma-$ray detectors : a Ge detector with a full energy range set to 1.8 MeV at a distance of 4.4 cm from the source and a Ge(Li) detector, which was placed 4.7 cm from the source position and had a full energy range of 4.0 MeV. A Si(Li) electron detector was also placed at the first detection station (G1) at a distance of 12 cm from the source. The e$^-$ detector was equipped with a mini-orange filter, which was placed between the source and the detector, leaving a distance of 4.5 cm between the detector and the filter. This placement of the mini-orange filter allowed for a peak in the efficiency curve for the electron detector at an energy of 750 keV.

The positions of these three detectors at the first counting station (G1) were such that the two $\gamma-$ray detectors were at 90°, and the electron detector was at 180° relative to one of the Ge detector.

A Ge detector and a Si(Li) electron detector were placed at the second counting station (G3). The Ge detector was placed 4.6 cm from the source position and had a full energy acceptance of 6.0 MeV. The electron detector was placed at 180° to the Ge detector at a distance of 7.0 cm from the source position.

This e$^-$ detector was also served by a mini-orange filter, which was placed 1.5 cm from the face of the detector and resulted in a peak efficiency curve for this detector at an energy of 250 keV.

Singles spectra were collected for each of the five detectors described above. Two-fold coincidences were collected between the two $\gamma-$ray detectors and the electron and Ge detectors at the first counting station (G1), and between the electron and Ge detectors at the second counting station (G3).

Examples of low-energy $\gamma-$ray and conversion electron spectra recorded at ISOLDE are shown in Figs. 1 and 2. Energies and intensities of the $\gamma-$rays associated to the ^{119}Cs decay are listed in Table 2. For both experiments at ISOLDE and at UNISOR the $\gamma-$ray intensities were determined relative to the 176.5 keV gamma-ray transition.

Efficiency curves were derived for each $\gamma-$ray detector using a standard reference source containing ^{154,155}Eu, ^{125}Sb and ^{125m}Te. Energy calibrations were performed by collecting $\gamma-$ray singles spectra for sources of ^{152}Eu and ^{228}Th with the simultaneous collection of the ^{119}Cs activities.

The experimental internal conversion coefficients are listed independently for the two series of measurements. Table 2 concerns low-energy $\gamma-$rays and a few intense transitions at intermediate energy studied at ISOLDE. The coefficients were estimated from singles spectra and normalized to the 176.5 keV, E1 transition, in agreement with its K/L experimental ratio. Table 3 concerns very low-energy transitions for which only L conversion lines were observed. The conversion coefficients measured at UNISOR for the more intense transitions in the decay of ^{119}Cs are listed in Table 4.

Table 3: Same as for Table 2 but for experimental and theoretical α_L internal conversion coefficients.

E_γ (keV)	α_L				Multipolarity
	exp	E1	E2	M1	
67.5	5 (2)	0.075	2.92	0.29	E2
68.0	0.9 (4)	0.073	2.78	0.29	M1
70.3	0.4 (1)	0.066	2.38	0.26	M1

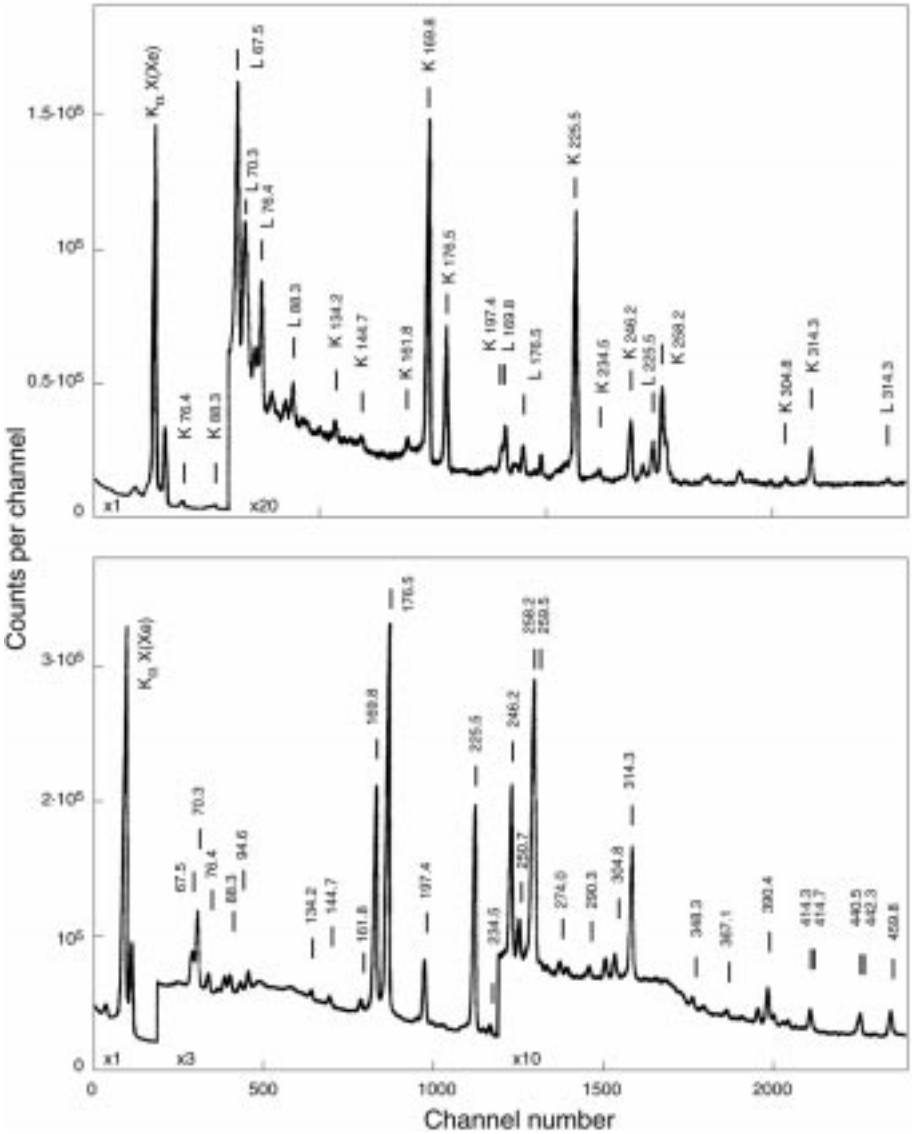

Figure 1: Partial conversion electron (upper panel) and gamma-ray (lower panel) spectra observed in the ^{119m,g}Cs decay at ISOLDE (collecting time 30 s, counting time 30 s).

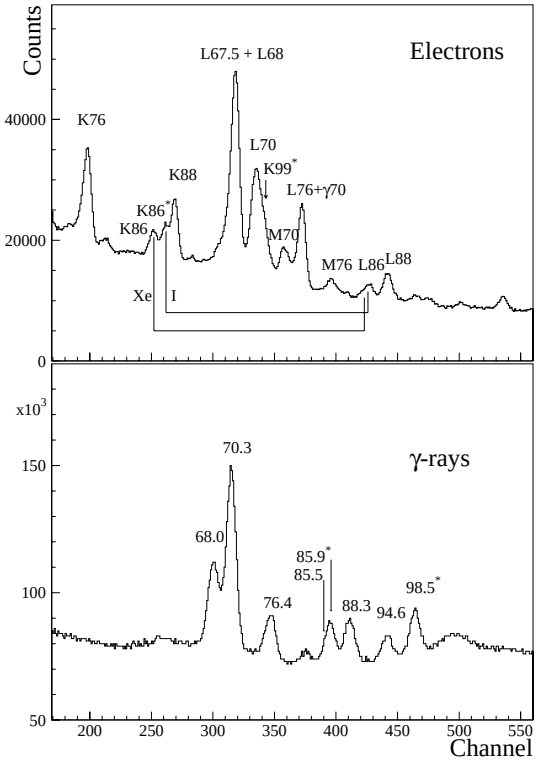

Figure 2: Expanded partial low-energy spectra for $\gamma-$rays (lower panel) and electrons (upper panel), recorded at ISOLDE in the ^{119m,g}Cs decay. They show the complexity of the spectra in the 50 to 100 keV energy range as well as the differences in transition multipolarities. Lines belonging to the decay of ^{119}Xe are labelled with *. Collecting time 1 s, counting time 30 s.

The electron intensities, for each transition, were determined using relative efficiency curves constructed using sources of ^{207}Bi and ^{133}Ba. The curves were normalized by considering the 176.5 keV, which has an E1 multipolarity. As mentioned above,the effect of the mini-orange filter was to peak the efficiency curve towards a specific electron window; the efficiency was peaked at 750 and 250 keV for the electrons in the first and the second stations, respectively.

While the existence of two long-lived species in ^{119}Cs was established and confirmed by many experiments, half-life evaluations are still scattered. The assignment of the $I^\pi = 9/2^+$ state to the ground-state was based on systematics of spins and magnetic moments in the odd-A cesium isotopes [3], [5].

For this state, a half-life $T_{1/2} = 43.0 \pm 0.2$ s is given in the Nuclear Data Sheets [15], in agreement with unpublished results [16]. Since the first evaluation $T_{1/2} = (33 \pm 8)$ s [17], other values have been successively reported: (37.7 ± 0.2) s [18], (44 ± 2) s [3], 36 s [5], (44 ± 3) s [6]. The situation is somewhat similar for the isomeric $I^\pi = 3/2^+$ state. A very precise half-life $T_{1/2} = (30.4 \pm 0.1)$ s is reported in the last compilations [15] while all the other experimental values appear somewhat smaller: 28 s [19], [5], (29 ± 2) s [3], [6].

The time spectra established in the present study for a large number of $\gamma-$rays belonging to ^{119}Xe give a set of half-life values from 29 s to 43 s, as shown in Fig. 3. After having established the ^{119}Xe level scheme fed simultaneously from the two long-lived ^{119m}Cs and ^{119g}Cs states (see section 3) this special situation is clearly understood. Indeed, as it will be presented later, a few high-spin ($I \geq 7/2$) excited levels in ^{119}Xe are

populated by the $I^{\pi} = 9/2^{+}$ ^{119g}Cs (see part (a) of Fig. 3) while the levels characterized by spin value I = 1/2, 3/2 or 5/2 are essentially fed by the $I^{\pi} = 3/2^{+}$ ^{119m}Cs isomer (see part (b) of Fig. 3). Obviously, in between these two extreme situations, as excited states which are not directly fed (or partially fed) by beta decay exist, many $\gamma-$rays in ^{119}Xe will exhibit intermediate half-lives. Two examples are shown in part (c) of Fig. 3 for the intense $\gamma-$rays at 169.8 keV and 197.4 keV which decay with a $T_{1/2} = (38 \pm 1)$ s half-life. Taking into account the collecting and counting times used in the present work and the complexity of the ^{119}Xe level scheme (discussed later in section 3) we estimate that it is very difficult to reach very precise half-life values. The following half-lives can be retained: $T_{1/2} = (43 \pm 1)$ s for the $I^{\pi} = 9/2^{+}$ ^{119g}Cs ground-state and $T_{1/2} = (29 \pm 1)$ s for the $I^{\pi} = 3/2^{+}$ ^{119m}Cs isomeric state. These results are in good agreement with those reported in the Nuclear Data Sheets compilations [15], except for the error estimations.

Finally the situation in ^{119}Cs is definitively very similar to the one already studied in ^{121}Cs [4]. The identification of two long-lived states I = 9/2 and I = 3/2 in both nuclei has been firmly established from on-line atomic beam magnetic resonance (ABMR) [19], [20] and by $\beta-$radiation detected optical pumping ($\beta-$RADOP) [21] experiments at ISOLDE. In both nuclei, the observation, by in-beam gamma spectroscopy [22] of $\Delta I = 1$ band structures built on the $9/2^{+}$ states associates a $9/2^{+}[404]$ πg9/2 Nilsson configuration for these states.

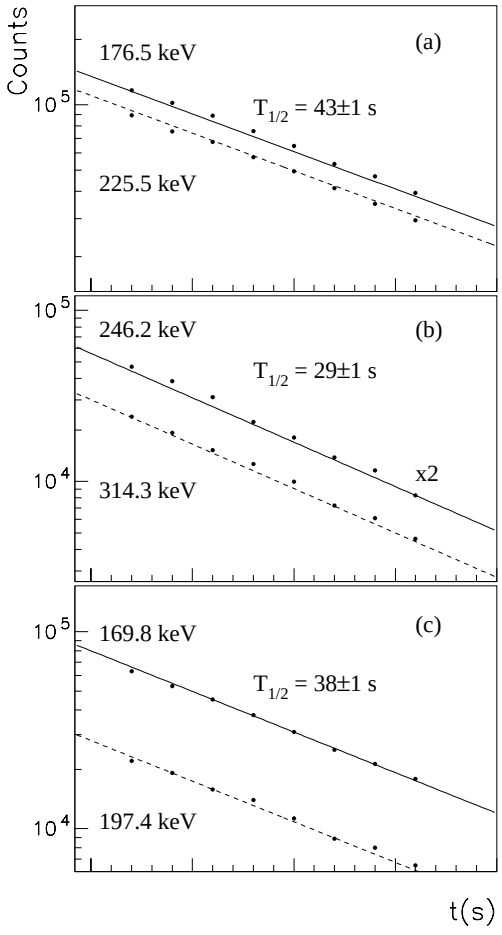

Figure 3: Examples of time spectra measured for several ^{119}Xe γ lines in the ^{119m,g}Cs decays. (a) : ^{119g}Cs decay, (b) : ^{119m}Cs decay, (c) : lines having a complex feeding.

From K and L conversion electron measurements, a direct 68.5 keV, $9/2^+ \rightarrow 3/2^+$ isomeric transition, with a M3 multipolarity has been identified in ^{121}Cs [4]. Obviously, a highly converted isomeric transition could appear in ^{119}Cs. However, no lines in coincidence with the K_α Cs X-rays, no conversion-electron lines from about 8 keV (energy limit in the spectra) to 50 keV and no very low-energy $\gamma-$rays were observed. In conclusion, if a highly converted M3 transition exists in ^{119}Cs with a branching of a few %, its energy would very likely be less than $10 - 15$ keV.

3 THE ^{119}Xe LEVEL SHEME

The ^{119}Xe level scheme obtained in the present work is shown in Figs. 4 (Part I), 5 (Part II) and 6 (Part III). It is based upon a $I^\pi = 5/2^+$ ground-state, previously identified as a $5/2^+[402]$ Nilsson neutron configuration [5]. The strongest $\gamma-$rays populated in ^{119}Xe have been used to establish the lowest excited states. The placement of the transitions has been determined by their coincidence relationships, their intensities (Table 1) and multipolarities (Table 2, 3 and 4). The $(\beta + \mathrm{EC})$ feedings have also added arguments for spin and parity assignments of several levels in ^{119}Xe (see Table 5 and next section). Figure 7, which contains only part of the ^{119}Xe level scheme extracted from our works, will be used in the following, instead of Figs. 4, 5 and 6, to discuss the results and assign the first members of several band structures, some of them being well observed and extended by in-beam spectroscopy studies.

The negative-parity group of levels, $7/2^-$, $11/2^-$, $9/2^-$, $13/2^-$, displayed at the right hand side of Fig. 7, is strongly fed from ^{119g}Cs. It deexcites to the $5/2^+$ ground-state via the strongest 176.5 keV, $7/2^- \rightarrow 5/2^+$, $\gamma-$ray which has an E1 multipolarity and is fed by the $T_{1/2} = 43$ s long half-life component of the ^{119}Cs $\beta-$decay (Fig. 3). These levels are similar to those previously identified as the $\nu h_{11/2}$ yrast band from in-beam measurements [7], [8], [9], [10]. In the present $\beta-$decay study a $\gamma-$ray at 68 keV was observed as a doublet which exhibits an intermediate half-life $T_{1/2} = 39$ s. However, from L-conversion electron spectra, it is possible to confirm the E2 multipolarity of a $11/2^- \rightarrow 7/2^-$, 67.5 keV transition (see Table 3) previously proposed in the first in-beam studies [7], [8].

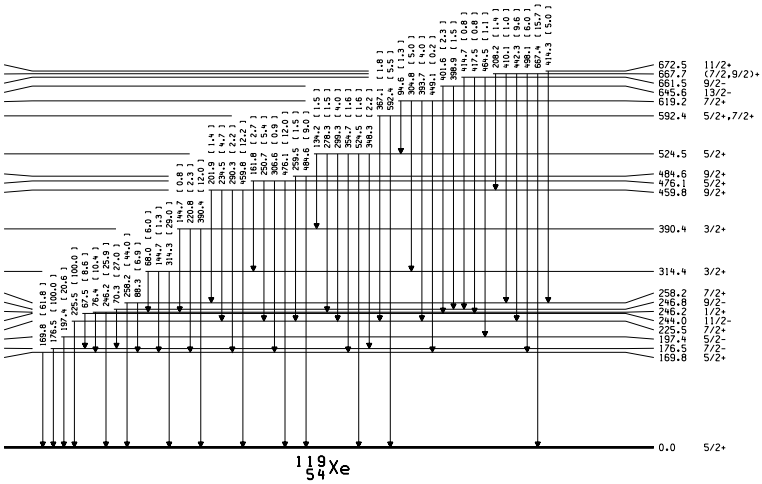

Figure 4: Partial level scheme in ^{119}Xe (Part I) showing the decay modes of excited states having energies up to 672.5 keV. Total transition intensities are given.

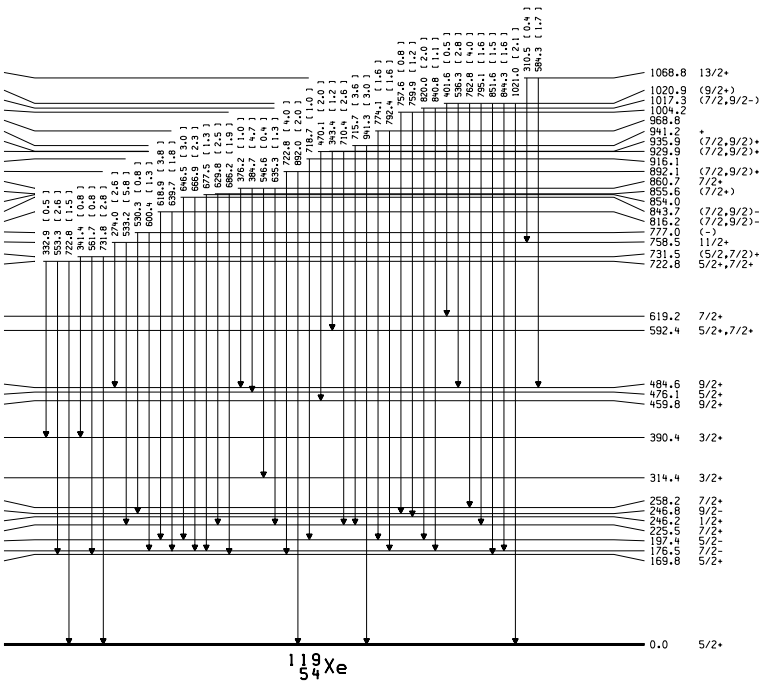

Figure 5: Same as Fig. 4 but for Part II of the ^{119}Xe level scheme showing the decay modes of excited states in the 700 to 1070 keV energy range. At low-energy excitations only states which are populated in the various decays are represented.

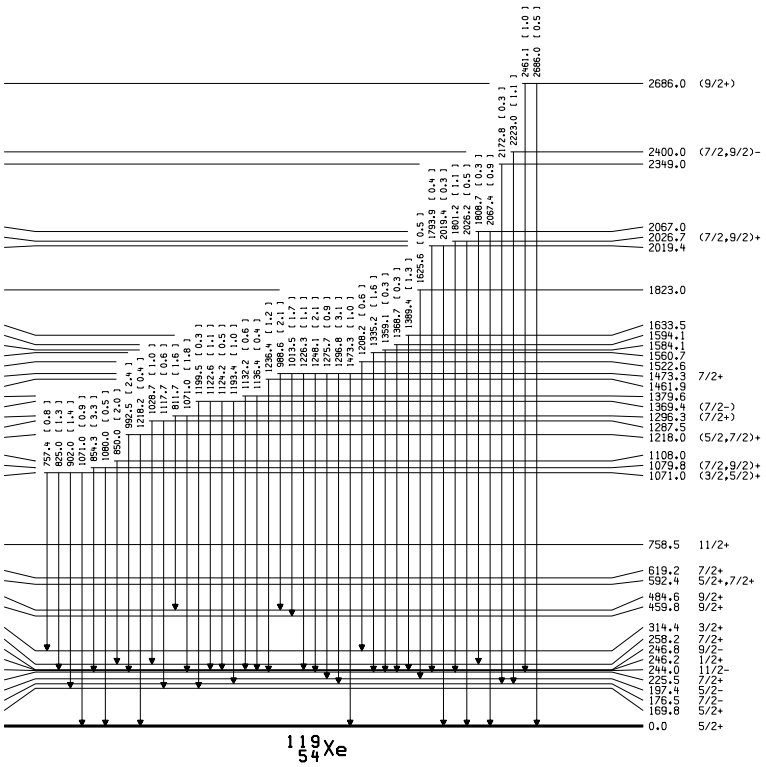

Figure 6: Same as Fig. 4 and 5 but for Part III of the ^{119}Xe level scheme showing the decay modes of excited states having energies larger than 1070 keV. At low-energy excitation only states which are populated in the various decays are represented.

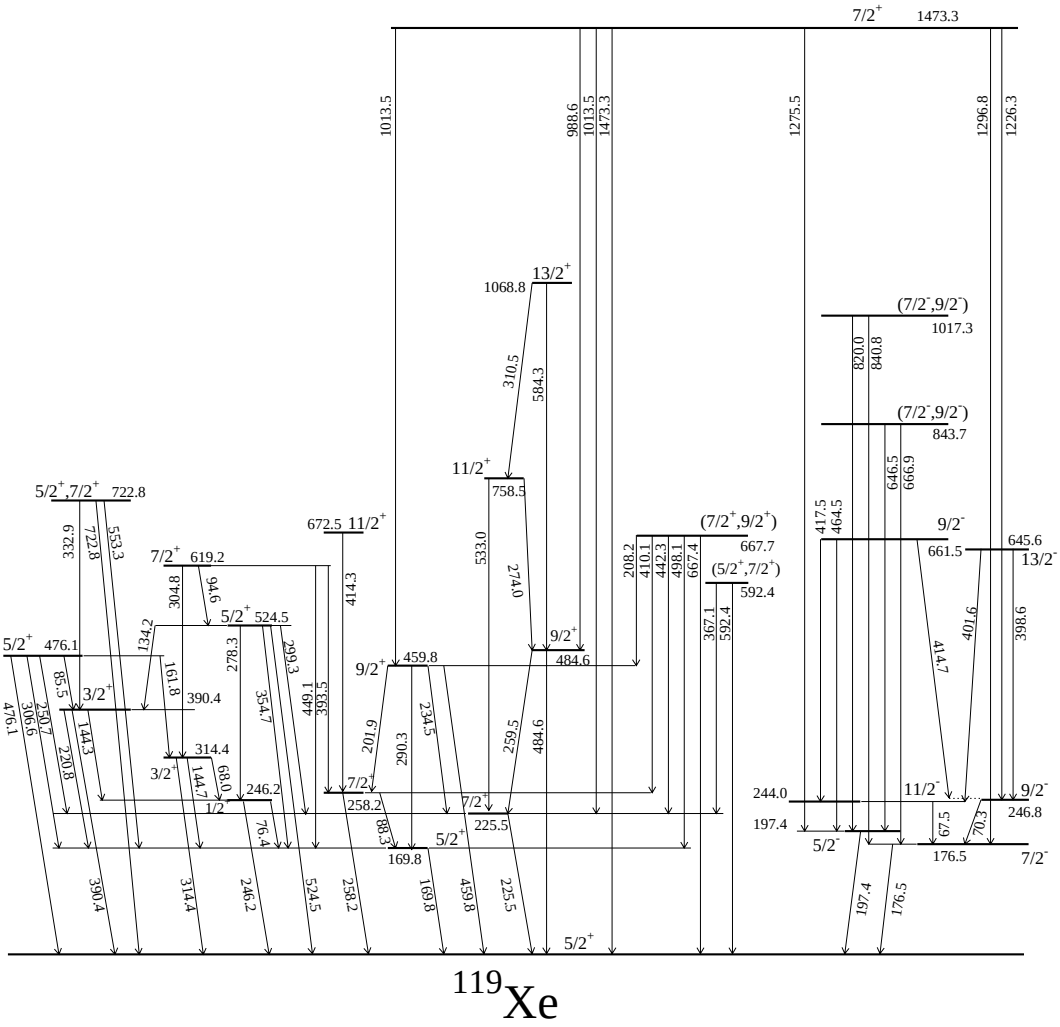

Figure 7: Low-energy part of the ^{119}Xe level scheme obtained in the ^{119m,g}Cs decay, showing the first members of band structures and their connexions. Transition and level energies are given in keV.

A M1 multipolarity is also confirmed for the $9/2^- \rightarrow 7/2^-$ 70.3 keV transition (Table 3) placed below the $9/2^-$ excited state at 246.8 keV. The $T_{1/2} = (23 \pm 4)$ ns determined from γ-$\gamma-$t time spectra for this $11/2^-$ excited state at 246.8 keV is in perfect agreement with the previous value of $T_{1/2} = (27 \pm 5)$ ns from in-beam data [8]. Several other new excited states are shown at the right-hand side of Fig. 7, all of them being established from $\gamma-\gamma$ coincidences. The level proposed at 197.4 keV deexcites to the $5/2^+$ ground-state via a strong γ transition observed with an intermediate half-life $T_{1/2} = (38 \pm 1)$ s and which has a E1 multipole character (Table 2). We propose to assign $I^\pi = 5/2^-$ to this state. It would correspond very likely to the $5/2^-$ [532] Nilsson neutron configuration expected for ^{119}Xe ($N = 65$) which has a Fermi level located in the middle of the $\nu h_{11/2}$ shell. A similar $5/2^-$ state was identified in the ^{121}Cs to ^{121}Xe decay [4] at 355.9 keV excitation energy, allowing the observation of both the $5/2^- \rightarrow 5/2^+$, E1 transition and the $5/2^- \rightarrow 7/2^-$, M1 transition at 159.7 keV. In the present work on ^{119}Xe, a $5/2^-$ to $7/2^-$ M1 transition of 21 keV has not been detected (see Fig. 7). However, the E1 multipolarity of the 197.4 keV transition is strongly in favour of a $I^\pi = 5/2^-$ assignment

at 197.4 keV and rejects the $I^\pi = (7/2^+, 9/2^+)$ excited state previously reported [15]. Due to their decay modes going essentially to the $5/2^-$, $7/2^-$, $9/2^-$ and $11/2^-$ states, a negative parity is proposed for several other excited states at 645.6 keV, 661.5 keV, 816.2 keV, 843.7, 1017.3 keV or 1369.4 keV (see Figs. 7, 4 and 5). Among them, only the $I^\pi = 13/2^-$ level at 645.6 keV has been confirmed by in-beam studies [8], [9], [10]. It corresponds to the lowest part of band 2 in Ref. [9] or band 6 in Ref. [10]. If one includes the $I^\pi = 5/2^-$ excited state observed in the present work, the two signature partners of the $\nu h_{11/2}$ $5/2^-[532]$ configuration are identified. The favored one (band 5 in Ref. [10]) is based on the $I^\pi = \Omega + 1 = 7/2^-$ state at 176.5 keV while the unfavored one (band 6 in Ref. [10]) starts on the $I^\pi = \Omega = 5/2^-$ band-head at 197.4 keV.

In the central part of Fig. 7 one easily sees the beginning of a band structure built upon the $I^\pi = 5/2^+$ ground-state and starting with the $7/2^+$ to $5/2^+$ transition at 225.5 keV. In the present work, this band is strongly fed from the ^{119g}Cs ($I^\pi = 9/2^+$) and observed up to the state $I^\pi = 13/2^+$ at 1068.8 keV. The cascade of M1 $\gamma-$rays at 225.5, 259.5, 274.0 and 310.5 keV is established as well as the E2 cross-over transitions at 484.6, 533.0 and 584.3 keV. This band structure, in complete agreement with in-beam data [8], [9], [10], is based on the $\nu d_{5/2}$ $5/2^+[402]$ Nilsson orbital previously established by laser spectroscopy measurements [5].

From the data presented on the left-hand side of Fig. 7 it appears that the level structure is relatively complex with many connexions between the various states. First, one can distinguish at the extreme left, two sets of states which are essentially fed by the ^{119m}Cs isomeric state ($I^\pi = 3/2^+, T_{1/2} = 29$ s). The most strongly populated band of this group is based upon the 246.2 keV state which mainly deexcites to the $5/2^+$ ground-state via a strong E2 transition (see Fig. 3, Part (b), and Table 2). From $\gamma-\gamma-$t coincidences a half-life of approximately 70 ns has been established for this 246 keV level in ^{119}Xe. In the ^{119}Cs decay, Westgaard et al. [23] observed a 246 keV transition which was considered later by Chowdhuryet al. [7] as the connexion between the $9/2^-$ state at 246.5 keV and the ^{119}Xe ground-state. This suggestion is completely rejected by γ and conversion electron spectra measured in the present experiment, and also by the tentative assignments proposed in Ref. [15] for the 246 and 314 keV excited states. The new positive-parity band shown in Fig. 7 which contains the states at 246.2, 314.4, 524.5, 619.2 keV with a probable extension up to the state at 1020.9 keV (see Fig. 5) can be based upo a $1/2^+$ state at 246.2 keV and is very likely dominated by the $s_{1/2}$ and $d_{3/2}$ neutron configurations. This band corresponds to the $1/2^+$ band recently identified in ^{121}Xe [4], starting at 153.9 keV and well populated in the ^{121}Cs beta decay. The second set of new excited states built upon a probable $(3/2^+)$ level at 390.4 keV exhibits a slightly collective character. It has relatively strong connexions and mixings with the sequence based on the $1/2^+$ state at 246.2 keV, the $5/2^+[402]$ ground-state rotational band and the $5/2^+$ state at 169.8 keV (discussed below).

It is more difficult to analyse the other positive parity states shown in Fig. 7 at 169.8, 258.2, 459.8 and 672.5 keV and also reported by in-beam data [7], [8], [9], [10]. The pure M1 character of the strong 169.8 keV transition supports spin and parity assignments $I^\pi = 5/2^+$ for the 169.8 keV excited state, in agreement with in-beam angular distribution studies [7], [9], [10]. The 76.4 keV, E2 line (Table 2) which connects the 246.2 keV $I^\pi = 1/2^+$ state and the 169 keV state supports also the same $I^\pi = 5/2^+$ assignment (see Fig. 7). As the $\nu d_{5/2}$ $5/2^+[402]$ Nilsson configuration can be retained for the ^{119}Xe ground-state in agreement with its magnetic moment, this excited state at 169.8 keV corresponds very likely to the $\nu g_{7/2}$ $5/2^+[413]$ configuration expected close to the Fermi surface for a neutron

number N = 65 at a deformation $\beta_2 \approx 0.2$. In the present work, the quality of conversion electron measurements is not good enough to reach very precise α_K values and K/L ratios for the transitions at 88.3, 201.9, 258.2 and 290.3 keV transitions (Table 2) and deduce firm I^π assignments. However, the pure M1 character observed for the 234.5 keV transition between states at 459.8 keV and 225.5 keV as well as the existence of cross-over transitions like those at 290.3 keV (201.9 + 88.6) or at 459.8 keV (234.5 + 225.5) can be considered in agreement with the in-beam data [10]. The states at 169.8, 258.2, 459.8 and 672.5 keV in Fig. 7 correspond to the first members of bands 1 and 2 in Ref. [10] which are given as two signature partners of the $\nu g_{7/2}$ $5/2^+$ [413] Nilsson configuration. Nevertheless, the strong $\gamma-$decay modes observed from the 459.8 keV state to the 225.5 keV ($7/2^+$) and to the $5/2^+$ ground-state show that it has a mixed nature. A similar conclusion concerns the excited state at 667.7 keV which deexcites strongly to the $5/2^+$ ground-state band but also to the members of the other positive-parity band built upon the 169.8 keV excited state. A configuration mixing is also reflected for the 1473.3 keV excited state which decays to the positive parity ground-state band, to the state at 459.8 keV but also to the $I^\pi = 7/2^-$ excited state at 176.5 keV.

4 $\beta-$FEEDINGS

From KX-ray intensities corrected for K-conversion rates and K-fluorescence yield [24], the electron capture intensities in ^{119m,g}Cs decays have been evaluated. Taking into account the $\gamma-$ray intensities given in Table 1, relative to I_γ(176 keV) = 1000, the total electron capture intensity is 1260 ± 300. Using the capture to positon ratio values for allowed branches tabulated by Gove and Martin [25] and the recent evaluated $\beta-$decay energy $Q(EC) = 6349$ keV for ^{119g}Cs to ^{119}Xe [26], we have calculated the total I(EC)+I(β) feedings for the known excited levels in ^{119}Xe from ^{119m}Cs and ^{119g}Cs to be $93 + 1227$ and $298 + 3122$, respectively. From the total annihilation quantum intensity we have estimated the total β intensity for the ^{119m,g}Cs decays. Our $\beta-\gamma$ coincidence measurement gives $I(\beta) = 8300 \pm 2000$, relative to I_γ(176 keV) = 1000. Under the experimental condition [13] the solid angle subtended by a centered source was 99.4% of 4π. In addition the collection times are short enough to neglect the long-lived components. This value is consistent with the previous result $I(\beta) = 6300 \pm 1050$ obtained by the coincidence method [23]. Due to the closeness of ^{119m}Cs and ^{119g}Cs half-lives, a complete separation of the two corresponding $\beta-$decays is excluded from the present work. Nevertheless, we have evaluated the ^{119g}Cs($9/2^+$)$\beta-$decay branches and apparent log ft values considering negligible feedings of the ^{119}Xe levels above 2.6 MeV and no $\beta-$decay branch to the ^{119}Xe ground-state (Table 5). Consequently only a rough estimate of the ^{119m}Cs($3/2^+$) to ^{119}Xe ground-state decay feeding has been made from total I(EC) and I(β) results. If we suppose the $\beta-$feeding to all the ^{119}Xe levels above 2.6 MeV as negligible, the EC + β branch from the ^{119m}Cs to the ^{119}Xe ground-state would be of about capture to positon ratio greater than 0.5, the EC + β branch to the ^{119}Xe ground-state would be about 43%. This leads to a log ft value from 5.0 to 5.3 for the EC + β^+ decay branch between the ^{119m}Cs($3/2^+$) and the ^{119}Xe ground-state ($5/2^+$). This result supports a $\Delta I = 1$ transition without parity change.

5 DISCUSSION OF THE RESULTS

The nuclei ^{119,121}Xe provide a suitable case for a fruitful comparison because a rich experimental data set is available for low-spin states via $\beta-$decay studies in addition to in-beam results.

5.1 Comparison of experimental results

As ^{119}Xe and ^{121}Xe have respectively 65 and 67 neutrons, the location of the Fermi energy is approximatively in the middle of the $h_{11/2}$ shell, in the upper part of the $g_{7/2}$ shell and near the $s_{1/2}$, $d_{3/2}$ and $d_{5/2}$ ones. According to this situation the ground-states of these two light odd-A xenon isotopes have been identified as $\nu d_{5/2}$, $5/2^+[402]$ configuration, on the basis of spin and parity and magnetic moment measurements [5]. Similarities exist also for energies and $\gamma-$decay modes of several low-lying positive-parity excited states. The situation is shown in Fig. 8 which contains the basic states of collective bands. The two first $I^\pi = 9/2^+$ states with their own $\gamma-$decay modes are also included. The existence of large configuration mixings in both the $9/2^+$ at 459.8 keV in ^{119}Xe and the $9/2^+$ at 706.2 keV in ^{121}Xe is clearly seen.

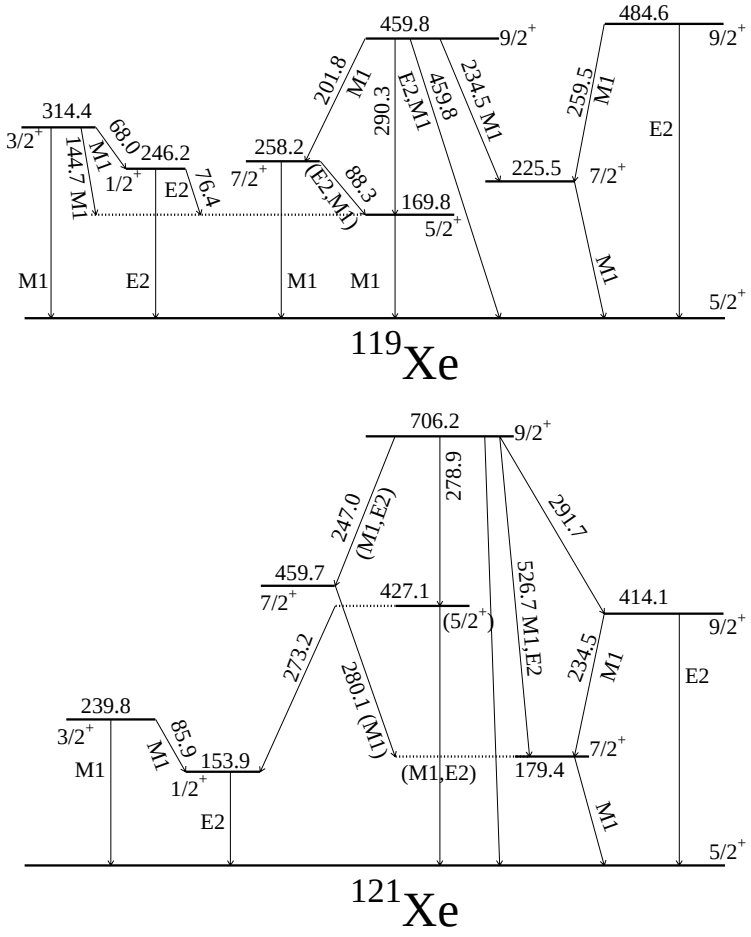

Figure 8: Comparison of positive-parity low-lying states in ^{119,121}Xe (from present work and Ref. 4).

The lower negative-parity states observed in the xenon isotopes with A = 117, 119 and 121 are the $I^\pi = 7/2^-$ states which decay via E1 transitions to the $5/2^+$ ground-states. The systematics presented in Fig. 9 illustrate the $\nu h_{11/2}$ level patterns and their connections to the $5/2^+$ ground-states. The spacings $15/2^- - 11/2^-$ appear very stable in these N = 63, 65 and 67 isotopes, from 400 keV in ^{117}Xe to 424 keV in ^{121}Xe, similarly to the $2^+ - 0^+$ spacings known in the neighbouring cores (472 keV in ^{118}Xe, 473 keV in ^{120}Xe and 497 keV in ^{122}Xe). The $5/2^-$ state appears at very low energy in ^{119}Xe but still

20.9 keV above the $7/2^-$ state contrary to the situation known in the N = 65 isotone ^{121}Ba where the $5/2^-$ state is 37 keV below the $7/2^-$ state [29] (see Fig. 10).

The comparison of the low-lying negative-parity states identified in the N = 65, ^{119}Xe and ^{121}Ba isotones illustrates also the different (β_2, γ) equilibrium deformations of the one-quasiparticule $\nu h_{11/2}$ near the ground-state of the light xenon and barium isotopes. Likewise somewhat different shapes for the favored and unfavored signatures of this $\nu h_{11/2}$ orbital have been discussed as function of N for xenon, barium and cerium [31].

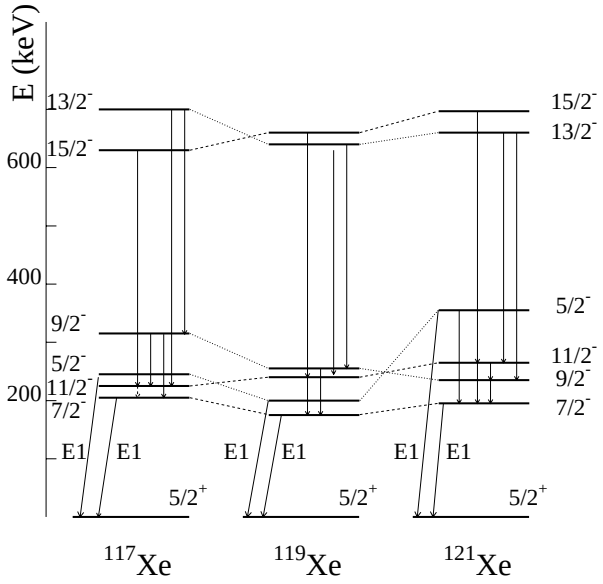

Figure 9: Comparison of negative-parity low-lying states identified in light xenon isotopes. Experimental data are from [6,27,28] for ^{117}Xe, [7-10] and the present work for ^{119}Xe, and [4,11,12] for ^{121}Xe.

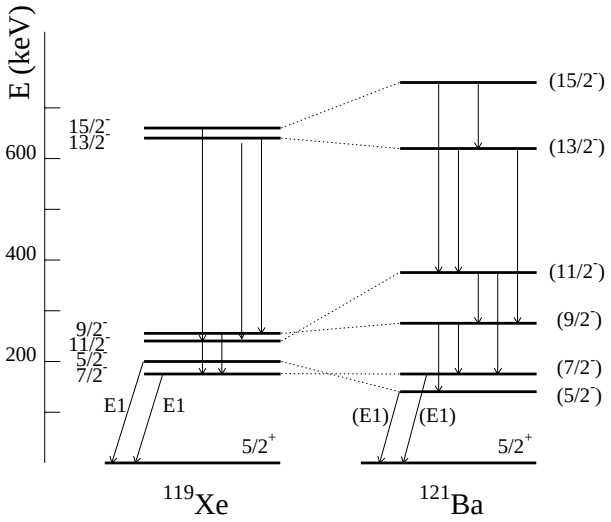

Figure 10: Comparison of negative-parity low-lying states identified in the N = 65 isotones of xenon and barium. Experimental data are from the present work and [7-10] for ^{119}Xe and [29-30] for ^{121}Ba.

5.2 IBFM calculations for ^{119}Xe

A description of the odd-mass xenon isotopes with A = 131 to 119 has been recently performed by multi-shell IBFM-1 calculations [32] similar to that reported for the barium isotopes [33]. Here we give only details concerning the ^{119}Xe nucleus. The procedure was to determine the values of the model parameters first for the heavier isotopes ($^{125-129}$Xe) where there are more experimental data, and keep these values or extrapolate them smoothly for the lighter isotopes. The quasiparticule energies and shell occupancies for ^{119}Xe were determined from a BCS calculation performed on a single-particle level scheme used also for ^{121}Xe [32]. The single-particule energies (in MeV) were $E(g_{7/2}) = 0.0$, $E(d_{5/2}) = 0.7$, $E(h_{11/2}) = 1.1$, $E(s_{1/2}) = 1.55$, $E(d_{3/2}) = 1.85$. In addition the $f_{7/2}$ and $h_{9/2}$ orbitals were set at about 3.2 MeV above the $h_{11/2}$ orbital. For the negative-parity states the boson-fermion interaction parameters are $A_0 = -0.21$ MeV, $\Gamma_0 = 0.56$ MeV and $\Lambda_0 = 1.87$ MeV whereas for the positive-parity states they are $A_0 = -0.12$ MeV, $\Gamma_0 = 0.21$ MeV and $\Lambda_0 = 0.46$ MeV. For the positive-parity states these values were also used for the heavier isotopes [32]. Since the assignment of some positive-parity states is somewhat uncertain, we have not tried any optimization of these parameters, but only verified that changes of up to $\pm 50\%$ in their values do not induce qualitative changes in the structure of the calculated bands. Figure 11 shows the experimental and calculated level schemes for positive-parity states. In comparing the results of the calculations with the experimental ones, one may count on several well established experimental facts : the single quasiparticule $d_{5/2}$ character of the ground-state, the four $\Delta J = 2$ bands labelled A, B, C and D with A and B being almost uncoupled, as well as the structure E which resembles the '$s_{1/2} + d_{3/2}$' band in the heavier isotopes [32].

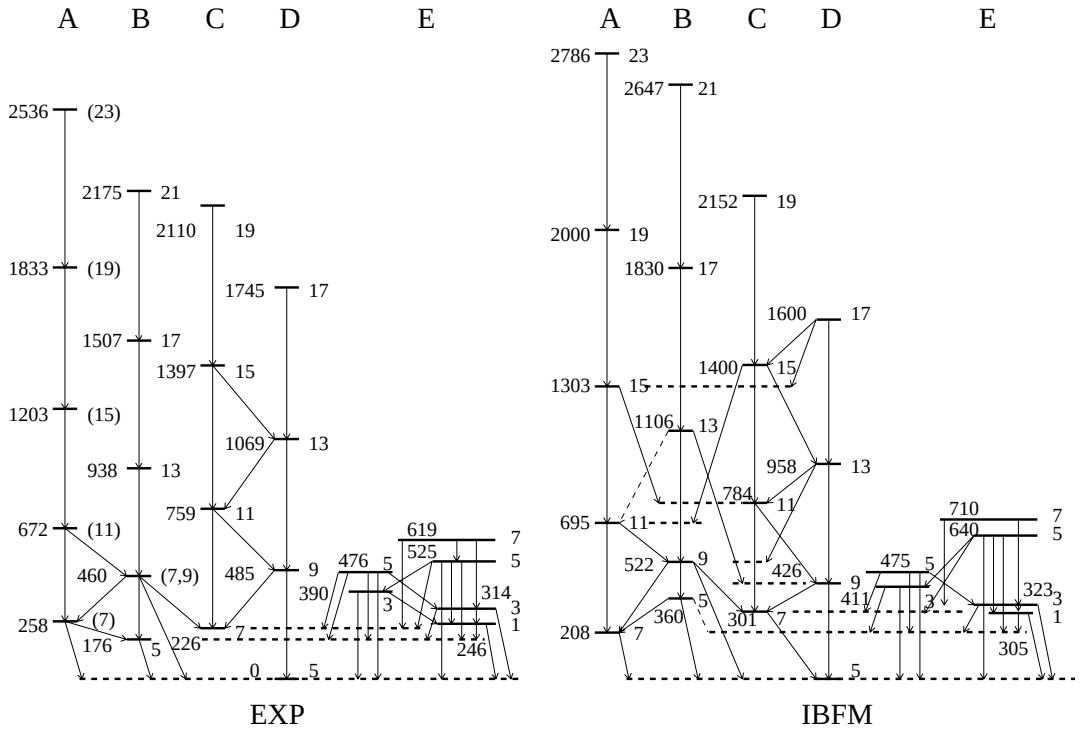

Figure 11: Comparison between the experimental and theoretical (IBFM) positive-parity level schemes. Gamma-ray decay branching ratios are given in Table 6. Spin values are multiplied by 2.

From Fig. 11 one can see that the calculations predict band structures which are rather similar to the experimental ones. The band structure labelled E is indeed found with configurations dominated by the $s_{1/2}$ and the $d_{3/2}$ orbitals. The state at 390 keV, $3/2^+$, is identified with a calculated one which is mainly a mixture between $d_{3/2}$ (21%) and $g_{7/2}$ (72%), whereas the 476 keV, $5/2^+$ level is a $d_{5/2} - g_{7/2}$ mixture with almost equal weights.

For the structures A to D we find configurations dominated by the $d_{5/2}$ and the $g_{7/2}$ orbitals, in most cases rather mixed, as it can be seen from Fig. 12 which shows the main composition of their wavefunctions in terms of the basis core states and quasiparticule orbitals. Thus, the configuration appears to be different from the heavier isotopes where one observes purer $d_{5/2}$ and the $g_{7/2}$ bands, respectively. In Ref. [8] it was emphasized that the recognition of the $d_{5/2}$ and the $g_{7/2}$ orbitals is difficult as their closeness in energy may cause them to mix strongly. Bands labelled 3 and 4 in Ref. [9] and in Ref. [10] which correspond to bands C and D in Fig. 11 were interpreted as based on the $5/2^+$ [402] configuration (originating in the $d_{5/2}$ spherical orbital), whereas bands A and B (assumed as $\Delta J = 2$ structures based on the state at 258.2 keV assigned as $7/2^+$, and 169.8 keV assigned as $5/2^+$, respectively) were labelled as bands 5 and 6 in Ref. [9] or bands 1 and 2 in Ref. [10] and considered as the two signature partners of the $5/2^+$ [413] configuration (originating in the $g_{7/2}$ spherical orbital). The calculations provide four such bands (Fig. 11) with a rather complex structure. The $5/2^+$ ground-state is predicted as a rather pure $d_{5/2}$ state, and its electric quadrupole moment of 1.31(5) b and magnetic dipole moment of $-0.6542(15)$ n.m. [34] are reasonably well predicted as $+0.572$ b and -0.64 n.m., respectively. The $5/2_2^+$ state is still dominated by the $d_{5/2}$ (69%) mixed with $g_{7/2}$ (22%). As it can be observed in Fig. 12, bands A and B start as rather pure $g_{7/2}$ bands, and C and D as rather pure $d_{5/2}$ bands, respectively. However, around spin 13/2, all these bands have a rather mixed $d_{5/2} - g_{7/2}$ character, after which the dominant orbitals change. At about this spin, the bands A and C, B and D, respectively, exchange their main configuration. The mixing that we get for the two orbitals ($d_{5/2}$ and $g_{7/2}$) may be somewhat too strong in certain states since we find some transitions between the bands that are not observed experimentally. Table 6 gives both the experimental and calculated branching ratios for some low-lying levels. The theoretical values were calculated using the same effective charge and gyromagnetic factor parameters as in the case of barium isotopes [33] and the experimental transition energies. Assuming a correspondence between experimental and calculated levels as shown by Fig. 11, the important decay branches are well accounted for. It is, nevertheless, impossible to draw strong conclusions on the assignment of all the experimental levels since there still remain discrepancies concerning the mixing ratios of some transitions. Thus, the 258.2 keV transition from the $7/2^+$ state in band A to the $5/2^+$ ground-state is calculated as 41% E2, which compares reasonably well with a value of at least 80% E2 (compatible with the measured internal conversion coefficients, Table). On the other hand, the 88.3 keV transition from the same level to the 169.8 keV $5/2^+$ one, is predicted as 97% M1 which does not fit with the E2, M1 mixed character found experimentally. Such discrepancies would appear to question the structure of the wavefunctions. On the other hand, it is known [33], [35] , that the standard M1 transition operator, which we have also used, may lead to difficulties in predicting M1 transitions quantitatively. Hence, one can only draw the conclusion that in this mid-shell nucleus, a strong mixing appears to take place between $d_{5/2}$ and $g_{7/2}$ orbitals in the structure of the observed bands, even at relatively low energies.

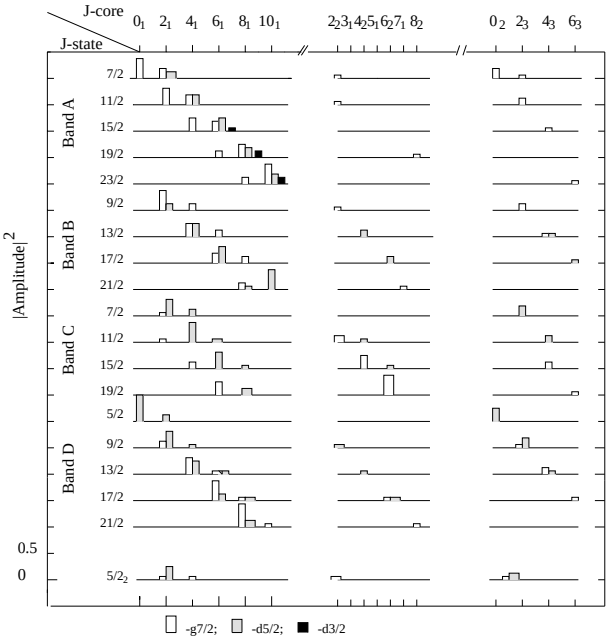

Figure 12: Composition of the IBFM wave functions of some positive-parity states for the bands A,B,C and D. Only the squared amplitudes larger than 5% are shown. J-core specifies the basis core states.

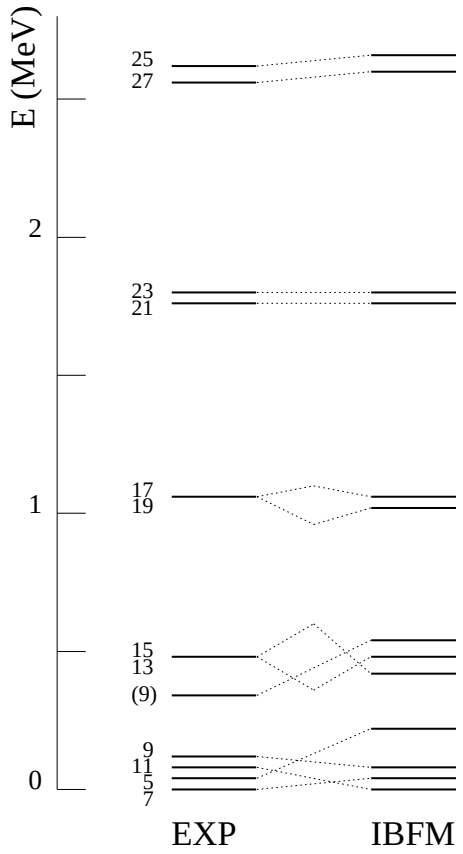

Figure 13: Comparison between the experimental and theoretical (IBFM) negative-parity level schemes.

The results of the calculations for the negative parity states are shown in Fig. 13. They are comparable with those of Ref. [8], the difference being that we use quasiparticule energies and shell occupancies which result from one BCS calculation performed for both the positive and negative states. All the calculated levels are dominated by the $h_{11/2}$ orbital. The strong staggering of the yrast band is well described, only the low-lying $5/2_1^-$ level is predicted somewhat higher.

6 SUMMARY

In the present work we have identified several new low-lying low-spin states in ^{119}Xe from the ^{119m,g}Cs $\beta-$decays. From multiscaling time spectra, half-lives of $T_{1/2} = (43 \pm 1)$ s for ^{119g}Cs ($I^\pi = 9/2^+$) and $T_{1/2} = (29 \pm 1)$ s for ^{119m}Cs ($I^\pi = 3/2^+$) have been revaluated with more realistic uncertainties than those obtained earlier. The basis of rotational structures have been observed up to $I^\pi = 13/2^-$ in the $5/2^-$ [532] band, to $I^\pi = 13/2^+$ in the $5/2^+$ [402] ground-state band, to $I^\pi = 11/2^+$ in the $5/2^+$ [413] band and to $I^\pi = 7/2^+$ in the '$s_{1/2} + d_{3/2}$' mixed structures. A comparison of the experimental negative-parity states is shown for the light xenon isotopes (A = 117, 119, 121) and for the N = 65 isotones ^{119}Xe and ^{121}Ba. Calculations performed in the boson-fermion interacting model for both parities describe reasonably well experimental features such as level energies and gamma-decay branching ratios.

7 ACKNOWLEDGEMENT

We express our gratitude to A. Knipper, J. Crawford and C. Richard-Serre for their interess and active participation in this work. One of us (DB) acknowledges the financial support from the French Romanian collaboration during stays at ISN Grenoble.

References

[1] J. Genevey-Rivier, A. Charvet, G. Marguier, C. Richard-Serre, J. D'Auria, A. Huck, G. Klotz, A. Knipper, G. Walter and the ISOLDE collaboration, Nucl. Phys. **A283**, 45 (1977).

[2] G. Marguier, A. Charvet, J. Genevey, C. Richard-Serre, A. Knipper, G. Walter and the ISOLDE collaboration, Nucl. Phys. **A342**, 301 (1980).

[3] J. Genevey, A. Charvet, G. Marguier, C. Richard-Serre, A. Knipper, J. Crawford and the ISOLDE collaboration, Proc. of the 4^{th}Int.Conf. NFFS, Helsingor, CERN Report 81-09, 483 (1981).

[4] J. Genevey, A. Gizon, G. Marguier, C. Richard-Serre, A. Knipper, P. Paris, C. F. Liang, B. Weiss and the ISOLDE and ISOCELE collaborations, Z. Phys. **A338**, 405 (1991).

[5] C. Thibault, F. Touchard, S. Buttgenbach, R. Klapisch, M. De Saint-Simon, H. T. Duong, P. Jacquinot, P. Juncar, S. Liberman, P. Pillet, J. Pinard, J. V. Vialle, A. Pesnelle and G. Huber, Nucl. Phys. **A367**, 1 (1981).

[6] G. Marguier, C. Richard-Serre, J. Genevey, M. Morgue, A. Charvet, J. Giroux, A. Huck, A. Knipper, G. Walter and the ISOLDE collaboration, J.Phys. G: Nucl. Phys. **12**, 757 (1986).

[7] P. Chowdhury, U. Garg, T. P. Sjoreen and D. B. Fossan, Phys. Rev. **C23**, 733 (1981).

[8] V. Barci, J. Gizon, A. Gizon, J. Crawford, J. Genevey, A. Plochocki and M. A. Cunningham, Nucl. Phys. **A383**, 309 (1982).

[9] V. P. Janzen, M. P. Carpenter, L. L. Riedinger, W. Schmitz, D. G. Popescu, J. A. Cameron, J. K. Johansson, D. D. Rajnauth, J. C. Waddington, G. Kajrys, S. Monaro and S. Pilotte, Phys. Rev. **C39**, 2050 (1989).

[10] H. C. Scraggs et al., Nucl. Phys. **A640**, 337 (1998).

[11] J. Timar, J. Simpson, E. S. Paul, S. Araddad, C. W. Beausang, M. A. Bentley, M. J. Joyce and J. F. Sharpey-Schafer, J. Phys. G: Nucl. Part. Phys. **21**, 783 (1995).

[12] C. B. Moon, T. Komatsubara, T. Shizuma, K. Uchiyama, Y. Sasaki and K. Furuno, Eur. Phys. J. **A4**, 107 (1999).

[13] F. K. Wohn, M.D. Glascock, W. L. Talbert, Jr., S. T. Hsue and R. J. Hanson, Phys. Rev. **C13**, 2492 (1976).

[14] R. Kirchner, K. H. Burkard, W. Hüller and O. Klepper, Nucl. Inst. Methods, **186**, 295 (1981).

[15] K. Kitao, M. Kanbe and K. Ogawa, Nucl. Data Sheets, **67**, 327 (1992) and S. Ohya, K. Kitao, Nucl. Data Sheets, **89**, 345 (2000).

[16] S. C. Ichikawa, T. Sekine, K. Hata, T. Tamura, E. Minchara, N. Takahashi, I. Fujiwara and N. Imanishi, Japan Atomic Energy Res. Inst. Tandem Ann. Rep. p. 60 (1984).

[17] J. Chaumont, E. Roeckl, Y. Nir-El, C. Thibault, R. Klapisch and R. Bernas, Phys. Lett. **29B**, 652 (1969).

[18] H. L. Ravn, S. Sundell and L. Westgaard, Phys. Lett. **39B**, 337 (1972).

[19] C. Ekström, G. Wannberg, J. Heinemeier and the ISOLDE collaboration, Phys. Lett. **B76**, 565 (1978).

[20] C. Ekström, S. Ingelman, G. Wannberg and M. Skarestad, Nucl. Phys. **A292**, 144 (1977).

[21] H. Fischer, P. Dabkiewicz, P. Freilinger, H. J. Kluge, H. Kremmling, R. Neugart and E. W. Otten, Z. Phys. **A284**, 3 (1978).

[22] U. Garg, T. P. Sjoreen and D. B. Fossan, Phys. Rev. **C19**, 217 (1979).

[23] L. Westgaard, K. Aleklett, G. Nyman and E. Roeckl, Z. Phys. **A275**, 127 (1975).
[24] Table of Isotopes, 7th ed., edited by C. M. Lederer and V. S. Shirley (Wiley, New York), 1978.
[25] N. B. Gove and M. J. Martin, At. Data Nucl. Data Tables **10**, 206 (1971).
[26] G. Audi, O. Bersillon, J. Blachot and A. H. Wapstra, Nucl. Phys. **A624**, 1 (1997).
[27] E. S. Paul, H. C. Scraggs, A. J. Boston et al., Nucl. Phys. **A644**, 3 (1998).
[28] Z. Liu, X. Sun, X. Zhou et al., Eur. Phys. J. **A1**, 125 (1998).
[29] B. Cederwall et al., Nucl. Phys. **A529**, 410 (1991).
[30] T. Sekine, S. Ichikawa, M. Oshima, H. Iimura, Y. Nagame, K. Hata, N. Takahashi and A. Yokoyama, Z. Phys. **A331**, 105 (1988).
[31] A. Granderath, P. F. Mantica, R. Bengtsson, R. Wyss, P. von Brentano, A. Gelberg and F. Seiffert, Nucl. Phys. **A597**, 427 (1996).
[32] Gh. Cata-Danil, D. Bucurescu, A. Gizon and J. Gizon, J. Phys. G: Nucl. Part. Phys. **20**, 1051 (1994).
[33] D. Bucurescu, Gh. Cata-Danil, N. V. Zamfir, A. Gizon and J. Gizon, Phys. Rev. **C43**, 2610 (1991).
[34] W. Borchers, E. Arnold, W. Neu, R. Neugart, K. Wendt, G. Ulm and the ISOLDE collaboration, Phys. Lett. **B216**, 7 (1989) and R. Neugart, private communication (1990)
[35] L. D. Wood and I. Morrison, J. Phys. **G15**, 997 (1989).

APPENDIX

Table 1: Energies in keV, relative intensities and location of $\gamma-$rays observed in the decay of ^{119m,g}Cs $\rightarrow$ ^{119}Xe. G1: First counting station, G3: Second counting station (see section 2).

Work at ISOLDE		Work at UNISOR			Location	
E_γ (keV)	$I_\gamma(\Delta I_\gamma)$	E_γ (keV)	$I_\gamma(\Delta I_\gamma)$ at G1	$I_\gamma(\Delta I_\gamma)$ at G3	From	To
67.5 (2)	10 (4)				244.0	176.5
70.3 (3)	82 (5)	70.9	95 (2)	169 (3)[1)]	246.8	176.5
76.4 (2)	18 (2)	77.1	19 (1)		246.2	169.8
85.5 (2)	6 (3)				476.1	390.4
88.3 (3)	19 (2)	88.0	17 (1)	32 (1)[1)]	258.2	169.8
94.6 (3)	13 (3)	95.0	16.6 (2)	14 (1)	619.2	524.5
134.2 (2)	15 (2)	134.5	15.1 (4)	12.2 (8)	524.5	390.4
144.3 (3)	8 (2)	144.2[4)]	8.5(6)	17.0(7)	390.4	246.2
144.7 (3)	10 (2)	145.1	10.1 (6)		314.4	169.8
161.8 (2)	22 (2)	162.1	22.6 (3)	15 (6)	476.1	314.4
169.8 (2)	520 (20)	169.8	516 (2)	520 (8)	169.8	0
176.5 (2)	1000 (40)	176.6	1000	1000	176.5	0
193.4 (3)	13 (4)	193.5	10.2 (6)	22 (3)		
197.4 (2)	200 (10)	197.4	199 (1)	209 (3)[1)]	197.4	0
201.9 (3)	14 (2)	202.1	15.2 (3)	16 (3)	459.8	258.2
205.8 (3)	11 (2)	206.1	7.0 (3)			
208.2 (2)	14 (2)	208.5	23.8 (4)	23 (2)	667.7	459.8
220.8 (2)	23 (3)	221.3[4)]	19 (1)	35 (4)	390.4	169.8
225.5 (2)	920 (30)	225.6	925 (2)	932 (7)	225.5	0
234.5 (2)	47 (5)	234.7	52.0 (9)	45 (4)	459.8	225.5
246.2 (2)	240 (15)	246.2	237 (1)	226 (3)	246.2	0
250.7 (3)	54 (5)	250.9	60.0 (6)	52 (2)	476.1	225.5
258.2 (3)	440 (30)	258.2	450 (2)	493 (4)	258.2	0
259.5 (3)	150 (20)	259.7	176 (1)	129 (3)	484.6	225.5
274.0 (3)	26 (3)	274.0	27.7 (5)	21 (2)	758.5	484.6
278.3 (3)	15 (2)	278.3	16.6 (4)	14 (2)	524.5	246.2
290.3 (3)	22 (2)	290.3	28.4 (5)	22 (2)	459.8	169.8
299.3 (2)	40 (4)	299.5	44.3 (6)	40 (2)	524.5	225.5
304.8 (3)	50 (4)	304.9	50.0 (4)	51 (2)	619.2	314.4
306.6 (2)	8 (2)	306.8	9.6 (2)		476.1	169.8
		310.5	3.6 (3)		1068.8	758.5
314.3 (2)	290 (20)	314.4	303 (2)	290 (3)	314.4	0
		332.9	5.0 (4)		722.8	390.4
		341.4	7.9 (3)		731.5	390.4
343.4 3)	≤ 3	343.4	11.9 (3)		935.9	592.4
348.3 (3)	22 (4)	348.3	29.9 (4)	21.2 (8)	524.5	176.5
354.7 (3)	16 (3)	355.1	17.1 (4)	14.6 (7)	524.5	169.8
367.1 (3)	17 (3)	367.6	21.6 (3)	17.9 (7)	592.4	225.5
376.2 (3)	10 (2)	376.3	14.4 (2)	10.3 (6)	860.7	484.6
384.7 (3)	47 (5)	385.0[4)]	50.5 (3)	47 (1)	860.7	476.1
390.4 (3)	120 (10)	390.4	131.2 (6)	121 (1)	390.4	0
393.5 (3)	40 (4)	393.8	43.0 (4)	39.2 (9)	619.2	225.5
398.9 (3)	15 (3)	399.1	18.9 (4)	14.8 (8)	645.6	246.8
401.6 (3)	23 (3)	402.1[4)]	28.2 (4)	23.2 (8)	645.6	244.0
401.6 (3)	5 (2)				1020.9	619.2
410.1 (3)	10 (2)	410.1	8 (1)	9.8 (8)	667.7	258.2
414.3 (3)	50 (10)	414.7[4)]	97.1 (6)	83.9 (9)	672.5	258.2
414.7 (4)	40 (10)				661.5	246.8
		417.5	8.3 (3)	8.4 (9)	661.5	244.0

Table 1: (Continued)

440.5(3)	19(3)					
442.3 (3)	95(10)	442.8	96.3 (9)	113 (2)[1)]	667.7	225.5
		449.1	2.1 (4)		619.2	169.8
		451.5	6.7 (9)	7 (1)		
459.8 (2)	122(10)	459.8	134 (1)	132 (2)	459.8	0
464.5 (3)	11 (2)	464.5	10.9 (8)		661.5	197.4
465.2 (3)	13 (3)	466.6	17 (1)	17 (1)[1)]		
470.1 (2)	20 (2)	470.4	22.8 (5)	19 (2)	929.9	459.8
476.1 (2)	105 (5)	476.1	134.4 (7)	123 (2)	476.1	0
484.6 (2)	90 (10)	484.9	125.0 (4)	101 (2)	484.6	0
498.1 (3)	60 (6)	498.6	83 (1)	60 (2)	667.7	169.8
518.6 (3)	17 (7)	519.0	25.3 (7)			
524.5 (3)	16(3)	524.5	23.9 (7)	16.4 (8)	524.5	0
		530.3	8.2 (5)	9.1 (7)	777.0	246.8
533.0 (2)	54 (3)	533.4	70.8 (6)	57.0 (7)	758.5	225.5
536.3 (3)	24 (3)	536.6	32.0 (5)	26.7 (7)	1020.9	484.6
546.6 (3)	12 (3)	547.1	18.2 (8)	12.4 (7)	860.7	314.4
553.3 (3)	26 (3)	553.7	33.6 (4)	25.5 (7)	722.8	169.8
561.7 (3)	10 (2)	561.0	8.5 (5)	11.6 (6)	731.5	169.8
580.7 (3)	9 (2)	581.4	13.2 (3)	13.2 (6)		
584.3 (3)	11 (3)	584.6	14.9 (4)	19.0 (6)	1068.8	484.6
592.4 (3)	55 (8)	592.9	67.4 (3)	55.5 (7)	592.4	0
595.8 (3)	12 (2)	596	14.5 (3)	12.9 (6)		
600.4 (3)	8 (3)	600.4	16.4 (3)	12.6 (7)	777.0	176.5
609.8 (3)	13 (2)	610.0	18.5 (2)	16.8 (9)		
		613.9	5.1 (2)	6.1 (8)		
618.9 (3)	36 (3)	618.9	37.6 (2)	38.8 (9)	816.2	197.4
629.8 (3)	25 (3)	630.1	31.4 (4)	25.4 (8)	855.6	225.5
635.3 (3)	11 (2)	635.6	12.5 (4)	14.6 (9)	860.7	225.5
639.7 (4)	13 (3)	639.7	21.2 (4)	18.0 (9)	816.2	176.5
646.5 (3)	30 (3)	647.1	39.1 (6)	26 (1)	843.7	197.4
		666.9	23.4 (7)		843.7	176.5
667.4 (3)	157 (15)	668.1	178 (1)	159 (1)[1)]	667.7	0
677.5 (3)	9 (2)	677.7	17.9 (2)	13.2 (9)	854.0	176.5
680.2 (3)	13 (3)	680.5	23.4 (3)	16.7 (9)		
		686.2	18.9 (4)		855.6	169.8
696.5 (3)	10 (2)	697.9	14.4 (2)	12 (1)		
710.4 (3)	26 (3)	710.8	27.6 (6)	26 (1)	935.9	225.5
715.7 (4)	36 (4)	716.4	42.1 (6)	39 (1)	941.2	225.5
718.7 (4)	10 (1)	719.2	11.6 (5)		916.1	197.4
722.8 (3)	15 (4)	722.9[4)]	65.1 (7)	54 (1)	722.8	0
722.8 (3)	40 (4)				892.1	169.8
731.5 (3)	30 (3)	731.8	32 (3)	25 (1)	731.5	0
757.2 (3)[4)]	15 (3)	756.7	9 (4)		1071.0	314.4
		757.6	13 (4)	15.7 (6)	1004.2	246.8
759.9 (3)	12 (3)	759.9	16 (3)	11.6 (6)	1004.2	244.0
762.8 (3)	31 (3)	763.3	50 (4)	47.4 (6)	1020.9	258.2
767.3 (3)	20 (2)	767.5	14 (3)	19.7 (3)[1)]		
771.4 (3)	16 (2)	770.8	12 (3)	18.6 (6)	968.8	197.4
774.0 (3)	18 (2)	774.7	17 (3)	16.2 (6)		
		787.3	4.9 (3)	4.8 (5)		
792.4 (3)	16 (2)	792.8	16.7 (3)	16.2 (5)	968.8	176.5
795.1 (3)	16 (2)	796.0	25.3 (3)	20.5 (5)	1020.9	225.5
		801.6	7.7 (2)	5.9 (4)		
811.7 (3)	8 (1)	811.6	21 (3)	16.7 (5)	1296.3	484.6

Table 1: (Continued)

820.0 (3)	16 (2)	820.0	27 (3)	20.3 (6)	1017.3	197.4
825.0 (3)	9 (2)	825.5	19 (3)	12.9 (6)	1071.0	246.2
832.5 (3)	10 (3)	832.7	17.0 (3)	13.3 (9)		
838.7 (3)	30 (3)	839.0	37.1 (3)	37.5 (9)		
		840.8	11.4 (3)		1017.3.	176.5
844.3 (3)	12 (2)	845.1	18.5 (3)	16.3 (8)	1020.9	176.5
		850.0	13.6 (3)		1108.0	258.2
851.6 (3)	15 (3)	852.3	14.6 (3)	21.3 (7)	1020.9	169.8
854.3 (3)	33 (3)	855.6	33.8 (3)	33.5 (8)	1079.8	225.5
		864.2	7.4 (2)	6.1 (7)		
867.8 (3)	3 (1)	868.6	7.9 (2)	8.2 (8)		
876.5 (3)	8 (1)	877.0	17.9 (3)	14.4 (9)		
892.0 (3)	13 (2)	891.8	23.2 (3)	16.9 (6)	892.1	0
898.4 (3)	4 (1)	898.8	8.6 (3)	5.7 (6)		
902.0 (3)	10 (2)	902.1	21.5 (3)	13.8 (6)	1071.0	169.8
931.2 (3)	w	930.9	8.6 (3)	5.0 (6)		
		935.9	9.6 (3)	8.3 (6)		
941.3 (3)	30 (3)	941.6	36.7 (4)	29.2 (6)	941.2	0
		949.2	8.5 (2)	8.7 (6)		
		959.7	4.0 (2)	3.0 (5)		
961.8 (3)	6 (2)	962.8	8.4 (2)	6.4 (5)		
988.6 (3)	21 (3)	988.6	27.2 (3)	22.6 (4)	1473.3	484.6
992.5 (3)	25 (3)	992.5	23.7 (3)	23.7 (4)	1218.0	225.5
996.9 (3)	8 (2)	997.0	8.3 (2)	8.0 (4)		
1013.5 (4)	17 (3)	1013.6	24.0 (3)	18.5 (5)	1473.3	459.8
1016.6 (4)	8 (2)	1016.7	9.3 (3)	5.7 (5)		
1021.0 (4)	21 (3)	1021.3	24.4 (4)	20.5 (5)	1020.9	0
1028.7 (4)	9 (1)	1029.2	16.4 (4)	10.3 (7)	1287.5	258.2
		1043.6	5.1(3)	3.3 (6)		
1049.9 (4)[3)]	6 (1)	1050.2	10.8 (3)	7.3 (6)		
1071.0 (3)[4)]	18 (3)	1071.0[4)]	36.7 (4)	28.7 (6)	1296.3	225.5
1071.0 (4)[4)]	9 (2)				1071.0	0
1080.0 (4)	4 (1)	1080.1	7.9 (3)	5.2 (6)	1079.8	0
1097.0 (4)	4 (1)	1097.0	9.7 (2)	7.3 (5)		
		1111.1	5.9 (2)	5.8 (5)		
		1117.7	11.6 (2)	10.9 (5)	1287.5	169.8
		1122.6	10.4 (2)	12.0 (5)	1369.4	246.8
1124.2 (4)	5 (1)	1125.3	5.5 (3)		1369.4	244.0
		1132.2	5.6 (3)	5.7 (5)	1379.6	246.8
1136.4 (4)	4 (1)	1135.9	9.2 (2)	9.7 (5)	1379.6	244.0
1157.0 (5)	3 (1)	1157.1	8.6 (3)	5.9 (6)		
1172.9 (4)	4 (2)	1171.8	8.5 (3)	6.7 (6)		
1193.4 (4)	10 (2)	1193.0	13.7 (3)	12.8 (6)	1369.4	176.5
1199.5 (5)	3 (2)	1199.5	10.1 (3)	8.5 (5)	1369.4	169.8
1208.2 (5)	6 (2)	1207.2	10.4 (3)	13.3 (5)[1)]	1522.6	314.4
1218.2 (5)	3 (1)				1218.0	0
		1220.0	5.4 (5)	8.0 (5)		
1226.3 (4)	11 (2)	1226.3	12.8 (3)	18.3 (6)	1473.3	246.8
1236.4 (4)	12 (2)	1236.4	16.2 (3)	14.4 (6)	1461.9	225.5
1248.1 (4)	21 (3)	1248.1	27.8 (3)	23.7 (6)	1473.3	225.5
1275.7 (4)	9 (2)	1275.7	6.0 (5)	4.9 (5)	1473.3	197.4
1296.8 (4)	31 (3)	1297.0	42.6 (6)	36.4 (5)	1473.3.	176.5
1306.1 (5)	4 (1)	1305.5	8.3 (3)	6.1 (5)		
		1309.7	8.6 (3)	6.2 (5)		
1335.2 (4)	16 (3)	1335.2	18.9 (3)	16.7 (6)	1560.7	225.5

Table 1: (Continued)

1353.3 (5)	5 (1)	1353.8	10.5 (2)	8.5 (5)		
1359.1 (4)	w	1359.1	5.0 (2)	5.5 (5)	1584.1	225.5
1368.7 (5)	w	1368.7	10.4 (2)	8.4 (5)	1594.1	225.5
		1379.6	9.4 (3)	7.6 (6)	(1379.6	0)
1389.4(5)	13 (3)	1389.4	16.5 ((4)	16.1 (6)	1633.5	244.0
		1396.8	5.7 (3)	3.1 (8)		
		1443.5	7.3 (3)	4.9 (7)		
1452.4 (5)	7 (2)	1452.8	12.6 (4)	11.0 (8)		
1473.3 (4)	10 (3)	1472.9	14.1 (3)	11.7 (6)	1473.3	0
		1476.1	6.7 (3)	4.9 (5)		
		1497.5	4.8 (3)	5.7 (5)		
1528.2 (4)	9 (3)	1528.2	13.2 (3)	11.3 (5)		
		1535.7	5.4 (2)	2.9 (6)		
		1540.5	7.3 (3)	7.1 (6)		
		1577.6	5.1 (3)	6.2 (6)		
		1589.8	4.7 (3)	4.5 (6)		
		1596.7	4.0 (3)	6.2 (6)		
1610.1 (5)	12(2)	1609.1	11.0 (3)	19.5 (6)[1)]		
		1616.1	4.5 (3)	5.1 (6)		
1625.6 (6)	5 (3)	1625.6	12.5 (3)	10.4 (7)	1823.0	197.4
		1701.5	5.4 (3)	3.3 (7)		
		1712.3	4.1 (3)	4.5 (7)		
		1752.9	4.6 (2)	4.8 (6)		
1767.2 (5)	w	1767.2	3.3 (2)	6.4 (2)		
		1773	3.3 (2)	2.8 (6)		
		1793.9	4.2 (3)	4.9 (6)	2019.4	225.5
1801.2 (6)	10 (2)	1801.2	13.7 (4)	20.2 (6)	2026.7	225.5
1808.7 (7)	w	1808.7	5.7 (3)	11.7 (6)[1)]	2067.0	258.2
		1814.0	4.0 (3)	5.6 (6)		
		1821.1	5.8 (3)	6.1 (6)		
		1833.3	3.5 (3)	7.4 (6)[1)]		
1850.9 (5)]	8 (2)	1850.3	10.0 (3)	14.1(7)		
		1916.4		5.2 (7)		
1983.8 (5)	6(2)	1983.8		11.8 (8)		
		2001.9		7.4 (8)		
		2019.4		2.8 (8)	2019.4	0
		2026.2		5.0 (8)	2026.7	0
		2067.4		8.6 (8)	2067.0	0
2172.8 (7)	w	2172.8		10.0 (9)	2349.0	176.5
		2184.3		5.4 (9)		
		2208.2		6.5 (9)		
		2219.6		5 (1)		
2223 (1)	11 (2)	2223.5		27 (1)	2400.0	176.5
2231 (1)	5 (1)	2232		11 (1)		
		2250.4		8 (1)		
		2260.0		6 (1)		
		2280.9		6 (1)		
		2303.8		8 (1)		
		2317.9		11 (1)		
		2461.1		10 (1)	2686.0	225.5
		2506.3		11 (1)		
		2529.3		7 (1)		
		2543.1		17 (1)		
		2655.2		9 (1)		
		2686.0		5.4 (9)	2686.0	0

Table 1: (Continued)

2718.3 (5)	w	2718.3	5 (1)
		2823.2	5 (1)
		2869.9	6 (1)
		2970.4	5 (1)
		3239.5	5 (1)

With the present experimental conditions the $\gamma-\gamma$ summing are negligible. Transitions not observed in coincidences or having gamma intensity smaller than 3 in the relative scale [$I_\gamma(176,5\ \text{keV}) = 1000$], are not reported in the present table.

[1)]The intensity reported may include intensity of an adjacent transition

[4)]Double line

w : Transitions observed in the measurement at ISOLDE but with intensities less than 4 in the relative scale

Table 2: Internal conversion electron data for transitions observed at ISOLDE in the decay of ^{119m,g}Cs $\rightarrow$ ^{119}Xe. This part of the table is for experimental and theoretical α_K coefficients and α_K/α_L ratios.

E_γ (keV)	α_K				α_K/α_L				Multipolarity
	exp	E1	E2	M1	exp	E1	E2	M1	
76.4	3.0(4)	0.38	2.73	1.55	1.7 (2)	7.36	1.68	7.58	E2
85.5	1.1(3)	0.28	1.96	1.12		7.44	2.01	7.61	M1
88.3	1.2(2)	0.26	1.78	1.02	2.3(3)	7.47	2.12	7.62	(E2,M1)
134.2	0.38(8)	0.08	0.47	0.31	$\geq$7	7.7	3.5	7.6	(M1)
144.7	0.20(5)	0.065	0.37	0.25	$\geq$7	7.7	3.7	7.6	M1
161.8	0.17(4)	0.048	0.26	0.18	$\geq$7	7.8	4.1	7.7	M1
169.8	0.17(4)	0.042	0.22	0.16	6.9(7)	7.8	4.2	7.7	M1+(E2)
176.5	[0.038]	0.038	0.19	0.15	7.2(8)	7.8	4.4	7.7	[E1]
197.4	0.030(3)	0.028	0.13	0.11	$\geq$7	7.8	4.7	7.7	E1
201.9	0.13(4)	0.026	0.12	0.10	$\geq$7	7.8	4.8	7.7	(M1)
225.5	0.079(5)	0.019	0.086	0.075	6.8(7)	7.9	5.1	7.7	M1+(E2)
234.5	0.062(2)	0.017	0.076	0.068	$\geq$7	7.9	5.2	7.7	M1
246.2	0.067(9)	0.015	0.065	0.060	5.5(9)	7.9	5.3	7.7	E2
250.7	0.064(9)	0.014	0.061	0.057	$\geq$7	7.9	5.4	7.7	(M1)
258.2	0.055(8)	0.013	0.056	0.052	5.7(3)	7.9	5.5	7.8	M1,E2
259.5	0.071(9)	0.013	0.055	0.052	$\geq$7	7.9	5.5	7.8	M1+(E2)
274.0	0.045(15)	0.011	0.046	0.045					M1,E2
299.3	0.025(8)	0.0091	0.034	0.036					M1,E2
304.8	0.030(7)	0.0086	0.033	0.034					(M1,E2)
314.3	0.037(5)	0.0080	0.030	0.031					M1,E2
390.2	0.021(4)	0.0046	0.015	0.018					M1,E2
414[4)]	0.017(5)	0.0040	0.013	0.015					M1,E2
442.3	0.012(3)	0.0034	0.011	0.013					M1,E2
459.8	0.008(3)	0.0031	0.0096	0.012					M1,E2
476.1	0.009(3)	0.0029	0.0087	0.011					M1,E2
484.6	0.009(3)	0.0027	0.0083	0.010					M1,E2
667.4	0.005(2)	0.0013	0.0036	0.0048					(M1,E2)

[4)] Double line

Table 4: Internal conversion electron data for transitions observed at UNISOR in the decay of ^{119m,g}Cs $\rightarrow$ ^{119}Xe. This part of the table is for experimental and theoretical α_K coefficients and α_K/α_L ratios. E_γ (keV) listed are those adopted in the ^{119}Xe level scheme.

E_γ (keV)	α_K					α_K/α_L				Multipolarity
	exp(P1)	exp(P2)	E1	E2	M1	exp(P1)	exp(P2)	E1	E2M1	
169.8		0.15(1)	0.042	0.22	0.16		11(2)	7.8	4.27.7	M1
176.5		0.039(1)	0.038	0.19	0.15		7.1(4)	7.8	4.47.7	E1
208.2		0.12(2)	0.024	0.11	0.093		9(3)	7.9	4.97.7	M1
220.8		0.06(2)	0.020	0.092	0.079			7.9	5.07.7	(M1)
225.5	0.070(2)	0.063(9)	0.019	0.086	0.075	5.7(2)	5.3(3)	7.9	5.17.7	M1+(E2)
234.5		0.067(10)	0.017	0.076	0.068			7.9	5.27.7	M1+E2
246.2	0.060(3)	0.063(9)	0.015	0.065	0.060	5.0(7)	5.4(4)	7.9	5.37.7	E2
250.7	0.068(10)	0.11(2)	0.014	0.061	0.057			7.9	5.47.7	(M1,E2)
258.2	0.059(4)	0.052()	0.013	0.056	0.052	8(2)	7(1)	7.9	5.57.8	M1
259.5	0.059(9)		0.013	0.055	0.052			7.9	5.57.8	M1,E2
274.0		0.031(3)	0.011	0.046	0.045			8.0	5.67.8	M1,E2
278.3		0.045(5)	0.011	0.044	0.043		3(2)	8.0	5.67.8	E2
290.3		0.080(7)	0.0098	0.038	0.039		10(4)	8.0	5.87.8	(M1,E2)
299.3	0.027(8)	0.025(2)	0.0091	0.035	0.036		6(3)	8.0	5.87.8	M1,E2
304.8	0.029(5)	0.027(2)	0.0086	0.033	0.034		5.6(13)	8.0	5.97.8	E2+(M1)
314.3	0.029(1)	0.027()	0.0080	0.030	0.031	9(3)	6.1(5)	8.0	6.07.8	M1+E2
348.3		0.0086(13)	0.0061	0.022	0.024			8.0	6.27.8	E1
367.1		0.015(2)	0.0054	0.019	0.021			8.0	6.37.8	E2,M1
384.7	0.020(3)	0.011(1)	0.0048	0.016	0.019			8.0	6.47.8	M1,E2
390.4	0.017(2)	0.012(1)	0.0046	0.015	0.018	10(3)		8.0	6.47.8	M1,E2
393.7	0.019(4)	0.012(1)	0.0045	0.015	0.018			8.0	6.47.8	M1,E2
414[4)]	0.012(1)	0.011(1)	0.0040	0.013	0.015		5.4(17)	8.1	6.57.9	E2,(M1)
442.3	0.012(1)		0.0034	0.011	0.013			8.1	6.67.9	E2,M1
459.8	0.00092(6)	0.0058(3)	0.0031	0.0096	0.012	5.4(16)		8.1	6.77.9	E2,M1
470.1		0.0087(17)	0.0029	0.0090	0.011			8.1	6.87.9	M1,E2
476.1	0.0087(11)	0.0067(4)	0.0029	0.0087	0.011	5(2)	5.1(13)	8.1	6.87.9	E2,M1
484.6	0.0064(5)	0.0062(4)	0.0027	0.0083	0.010	3(2)	3(1)	8.1	6.87.9	E2
498.1	0.0078(6)	0.0078(6)	0.0026	0.0077	0.0098					E2+(M1)
533.2	0.0075(5)	0.0087(8)	0.0022	0.0064	0.0083					E2,M1
553.3	0.0056(8)	0.0047(14)	0.0020	0.0058	0.0076					E2,M1
592.4	0.0044(3)	0.0061(10)	0.0017	0.0048	0.0064					E2,M1
618.9	0.0037(3)	0.0043(9)	0.0016	0.0043	0.0058					E2,M1
667.4	0.0044(16)	0.0041(3)	0.0013	0.0036	0.0048					M1,E2
710.4	0.0034(4)		0.0012	0.0031	0.0041					E2,M1
715.7	0.0034(3)		0.0012	0.0030	0.0041					E2,M1
722.8[4)]	0.0029(2)	0.0029(8)	0.0011	0.0029	0.0040					E2,M1
731.5	0.0022(4)		0.0011	0.0029	0.0039					E2,M1
762.8	0.0042(4)	0.0042(9)	0.0010	0.0026	0.0035					M1,E2
820.0	0.0017(5)	0.0059(21)	0.0009	0.0022	0.0030					(M1,E2)
854.3	0.0013(3)		0.0008	0.0020	0.0027					(E2,M1)
902.0	0.0015(4)		0.0007	0.0018	0.0024					E2,M1
1071.0	0.0013(4)		0.0005	0.0012	0.0016					E2,M1
1335.2	0.0024(8)		0.0004	0.008	0.0010					(M1)

Table 5: (EC+β^+) feedings and apparent log ft values for selected levels in the ^{119g}Cs decay.

Level (keV)	I(EC + β^+)%	log ft
2686	0.4	6.3
2400	0.3	6.5
2349	0.1	7.0
2067	0.3	6.7
2026.7	0.5	6.5
2019.4	0.2	6.9
1823	0.2	7.0
1633.5	0.4	6.8
1594.1	0.1	7.4
1584.1	0.1	7.4
1560.7	0.5	6.8
1522.6	0.2	7.2
1473.3	3.5	5.9
1461.9	0.3	7.0
1379.6	0.3	7.1
1369.4	0.8	6.6
1296.3	0.8	6.7
1287.5	0.6	6.8
1218.0	0.4	7.0
1108.2	0.4	7.1
1079.8	1.1	6.6
1068.8	0.4	7.1
1020.9	3.6	6.1
1017.3	0.9	6.7
1004.2	0.7	6.9
968.8	0.9	6.8
941.2	1.9	6.5
935.9	0.8	6.8
929.9	0.6	7.0
916.1	0.3	7.3
892.1	1.6	6.5
860.7	2.4	6.4
855.6	1.3	6.7
854.0	0.3	7.3
843.7	1.6	6.6
816.2	1.6	6.6
777.0	0.5	7.1
758.5	2.3	6.4
731.5	0.7	7.0
722.8	0.7	7.0
672.5	1.5	6.7
667.7	9.9	5.8
661.5	1.7	6.6
645.6	1.1	6.8
619.2	3.4	6.3
592.4	1.0	6.9
484.6	4.4	6.3
459.8	4.6	6.3
258.2	11.1	6.0
246.8	4.8	6.3
244.0	0.8	7.1
225.5	6.1	6.2
176.5	15.0	5.9

Table 6: Experimental and calculated branching ratios for some low-lying positive-parity states in ^{119}Xe. Calculated branchings below 1 are given only if observed experimentally. Unobserved branchings are marked with "u".

				Branching ratios	
J_i	E_i (keV)	J_f	E_f (keV)	Exp.	Calc.
$1/2_1$	246.2	$5/2_1$	0	100(6)	100
		$5/2_2$	169.8	7(1)	0.2
$3/2_1$	314.4	$5/2_1$	0	100(7)	100
		$1/2_1$	246.2	7(2)	< 0.1
$3/2_2$	390.4	$5/2_1$	0	100(8)	100
		$5/2_2$	169.8	19(3)	9
		$1/2_1$	246.2	7(2)	0.2
$5/2_3$	476.1	$5/2_1$	0	194(9)	85
		$5/2_2$	169.8	15(4)	127
		$3/2_1$	314.4	41(4)	2
		$7/2_1$	225.5	100(10)	100
		$7/2_2$	258.2	u	8
$5/2_4$	524.5	$5/2_1$	0	100(19)	100
		$5/2_2$	169.8	100(19)	73
		$1/2_1$	246.2	94(13)	11
		$3/2_2$	390.4	94(13)	1
		$7/2_1$	225.5	250(25)	4
$7/2_1$	225.5	$5/2_1$	0	100(3)	100
		$5/2_2$	169.8	u	3
$7/2_2$	258.2	$5/2_1$	0	100(7)	100
		$5/2_2$	169.8	4(1)	9
$7/2_3$	619.2	$5/2_1$	0	u	11
		$5/2_2$	169.8	4(1)	5
		$5/2_3$	476.1	u	3
		$5/2_4$	524.5	26(11)	< 0.1
		$3/2_1$	314.4	100(8)	100
		$7/2_1$	225.5	80(8)	87
		$7/2_2$	258.2	u	5
		$9/2_1$	459.8	u	17
		$9/2_2$	484.6	u	27
$9/2_1$	459.8	$5/2_1$	0	100(9)	100
		$5/2_2$	169.8	18(2)	2
		$7/2_1$	225.5	38(4)	17
		$7/2_2$	258.2	11(2)	10
$9/2_2$	484.6	$7/2_1$	225.5	100(13)	100
		$5/2_1$	0	60(6)	600
$11/2_1$	672.5	$7/2_2$	258.2	100(20)	100
		$9/2_2$	484.6	u	2
$11/2_2$	758.5	$7/2_1$	225.5	100(6)	100
		$9/2_2$	484.6	48(6)	4